Impact of an oblique breaking wave on a wall

Jian-Jun Shu
School of Mechanical & Production Engineering, Nanyang Technological University, 50 Nanyang Avenue, Singapore 639798

(Received 11 April 2003; accepted 20 November 2003; published online 29 January 2004)

The intention of this paper is to study impact force of an oblique-angled slamming wave acting on a rigid wall. In the present study the analytical approach is pursued based on a technique proposed by Shu (Proceedings of the International Conference on Applied Mathematics & Mathematical Physics, Sylhet, Bangladesh, 2000). A nonlinear theory in the context of potential flow is presented for determining accurately the free-surface profiles immediately after an oblique breaking wave impingement on the rigid vertical wall that suddenly starts from rest. The small-time expansion is taken as far as necessary to include the accelerating effect. The analytical solutions for the free-surface elevation are derived up to the third order. The results derived in this paper are of particular interest to the marine and offshore engineering industries, which will find the information useful for the design of ships, coastal and offshore.
[DOI: 10.1063/1.1644145]

I. INTRODUCTION

One of the most devastating forces of nature is that of breaking waves. The destructive force of breaking waves is economically and physically detrimental and fatal. Hence, a considerable amount of research has been devoted to the study of the impact forces of breaking waves, particularly that of breaking waves impacting on a rigid wall, which is suddenly started from rest and made to move towards a fluid jet. Such studies can yield useful results that would benefit designers of dams, ships, oil rigs, and other coastal and offshore structures, which are directly subjected to the impact forces of breaking waves.

When a breaking wave strikes a wall, the impact produced is of short duration but considerable intensity. This direct collision generates an impulsive pressure on the wall, which is similar to the problem of initial-stage water impact. However, existing wave theories based on small and finite amplitude assumptions cannot accurately model the breaking wave force on a wall due to the highly nonlinear and transient nature of the problem.

In reviewing the previous studies, one of the most important and unresolved questions is how the initial stage of the breaking wave impingement on the wall can be properly characterized and simulated. Cumberbatch[1] considered the case of symmetric normal impact of a water wedge on a wall, and Zhang *et al.*[2] took it further by studying an oblique impact. These two works assumed prescribed functions of the free-surface profiles close to the wall: in Cumberbatch,[1] a linear function was assumed while in Zhang *et al.*,[2] an exponential function was assumed. These two works were stemmed from an *ad hoc* assumption on the free-surface profiles close to the wall.

In Shu,[3] an analytical approach was taken to solve the breaking wave problem for a normal wave without prescribed functions. It has been found that the free-surface profile close to wall is neither linear in Cumberbatch's assumption[1] nor exponential in Zhang *et al.*'s assumption.[2] This paper aims to take the same analytical approach, but instead of a normal wave, we shall derive and solve the impact problem due to an oblique angled wave.

In the present study, we do not assume any prescribed functions for the free-surface profiles. Effects of gravity, viscosity, and surface tension can be neglected since inertia forces are dominant during the small-time impact process. The essential mechanism involved in the impact process can be described by the theoretical treatment of potential flow. A small portion of the breaker tip is initially cut off to produce a finite wetted area on the wall and a high spike in the consequent impact results from an acceleration of water towards the wall. We are interested in the short time successive triggering of the nonlinear effects using a small-time expansion of the full, nonlinear initial/boundary value problem.

II. GOVERNING EQUATIONS

We consider a rigid horizontal wall, being suddenly started from rest and made to move vertically with constant acceleration a_0 (vertical component $a_y=a_0\cos\beta$) towards a two-dimensional fluid truncated wedge with semiangle $\alpha\pi$ $(0<\alpha<\frac{1}{2})$. A definition sketch of the flow is shown in Fig. 1. The axis of the fluid truncated wedge is at an angle $\beta\pi$ $(0<\beta<\frac{1}{2}-\alpha)$ to the vertical. Let me nondimensionalize time t by $(L_2/a_y)^{1/2}$, distance (x,y) by L_2, velocity (u,v) by $(a_yL_2)^{1/2}$, pressure p by ρa_yL_2, where L_1 and L_2 are the right-side and left-side wetted wall semilengths, respectively, when the breaking wave just touches the wall at time $t=0$ and ρ is the density of the fluid. A mathematical statement of the above problem can now be written as

$$\frac{\partial u}{\partial x}+\frac{\partial v}{\partial y}=0, \tag{1}$$

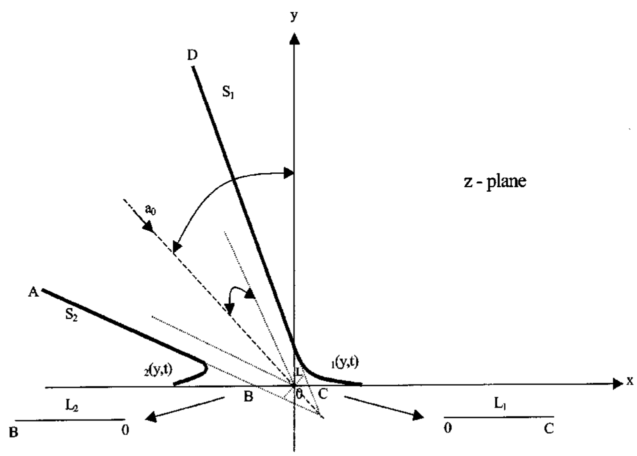

FIG. 1. A sketch of fluid body in physical z plane showing the free-surface "elevations" η_1 and η_2 at the instant of shortly after impact.

$$\frac{\partial u}{\partial t}+u\frac{\partial u}{\partial x}+v\frac{\partial u}{\partial y}=-\frac{\partial p}{\partial x}, \tag{2}$$

$$\frac{\partial v}{\partial t}+u\frac{\partial v}{\partial x}+v\frac{\partial v}{\partial y}=-\frac{\partial p}{\partial y}. \tag{3}$$

For negative time $t<0$ everything is at rest,

$$u=v=0, \quad \eta_1=0, \quad \eta_2=0 \quad \text{for } t<0, \tag{4}$$

where η_1 and η_2 are the free-surface "elevations" in the x direction beyond the undisturbed surfaces. On the surfaces, the kinematic and dynamic boundary conditions require

$$u=\frac{\partial \eta_1}{\partial t}+v\frac{\partial \eta_1}{\partial y},$$

$$p=0 \quad \text{on} \quad x=\lambda+y\tan[(\alpha-\beta)\pi]+\eta_1(y,t), \tag{5}$$

$$u=-\frac{\partial \eta_2}{\partial t}-v\frac{\partial \eta_2}{\partial y},$$

$$p=0 \quad \text{on} \quad x=-1-y\tan[(\alpha+\beta)\pi]-\eta_2(y,t), \tag{6}$$

where the dimensionless number λ can be expressed in the terms of angles $\alpha\pi$ and $\beta\pi$ as follows:

$$\lambda=\frac{L_1}{L_2}=\frac{\cos[(\alpha+\beta)\pi]}{\cos[(\alpha-\beta)\pi]}. \tag{7}$$

On the wall surfaces, the normal velocity of fluid particles must be the same as that of the wall at all the time

$$v=a_y t \quad \text{on} \quad y=\tfrac{1}{2}a_y t^2. \tag{8}$$

The pressure vanishes at infinity,

$$p\to 0 \quad \text{as} \quad y\to\infty. \tag{9}$$

The solution domain for this set of Eqs. (1)–(3) with conditions (4)–(9) is unknown at this stage of the analysis but is conveniently described as

$$\Big\{(x,y,t): -1-y\tan[(\alpha+\beta)\pi]-\eta_2(y,t) \le x \le \lambda+y\tan[(\alpha-\beta)\pi]+\eta_1(y,t), \quad \frac{1}{2}a_y t^2 \le y<\infty, \quad 0\le t<\infty\Big\}.$$

III. MATHEMATICAL ANALYSIS

The full nonlinear initial/boundary value problem consists of Eqs. (1)–(3) with conditions (4)–(9). These equations are solved analytically by employing a small-time expansion.[4–7] We assume that

$$u(x,y,t)=u_1(x,y)t+O(t^2), \quad v(x,y,t)=v_1(x,y)t+O(t^2), \tag{10}$$

$$p(x,y,t)=p_0(x,y)+O(t), \tag{11}$$

$$\eta_1(y,t)=\eta_{12}(y)t^2+O(t^3), \quad \eta_2(y,t)=\eta_{22}(y)t^2+O(t^3). \tag{12}$$

The leading-order equations are

$$\frac{\partial u_1}{\partial x}+\frac{\partial v_1}{\partial y}=0, \quad u_1=-\frac{\partial p_0}{\partial x}, \quad v_1=-\frac{\partial p_0}{\partial y} \tag{13}$$

subject to the conditions

$$u_1=2\eta_{12}, \quad p_0=0 \quad \text{on} \quad x=\lambda+y\tan[(\alpha-\beta)\pi], \tag{14}$$

$$u_1=-2\eta_{22},$$

$$p_0=0 \quad \text{on} \quad x=-1-y\tan[(\alpha+\beta)\pi], \tag{15}$$

$$v_1=a_y \quad \text{on} \quad y=0, \tag{16}$$

$$p_0\to 0 \quad \text{as} \quad y\to\infty. \tag{17}$$

It is clear that pressure p_0 satisfies the Laplace equation

$$\frac{\partial^2 p_0}{\partial x^2}+\frac{\partial^2 p_0}{\partial y^2}=0. \tag{18}$$

Introducing a complex-conjugate function q_0 with respect to p_0, we can construct an analytic function

$$f_0(z)\equiv p_0+iq_0, \quad z=x+iy. \tag{19}$$

As shown in Fig. 2, the conformal mapping

$$z=-1+\frac{(1+\lambda)\Gamma(1+2\alpha)}{\Gamma(1+\gamma_1)\Gamma(1+\gamma_2)}\int_0^w \tau^{\gamma_2}(1-\tau)^{\gamma_1}d\tau \tag{20}$$

given by the Schwarz–Christoffel transformation, maps the upper half of the w plane ($w=\xi+i\zeta$) onto the region occupied by the fluid. Here Γ is the Gamma function defined by

$$\Gamma(w)=\int_0^\infty \tau^{w-1}e^{-\tau}d\tau.$$

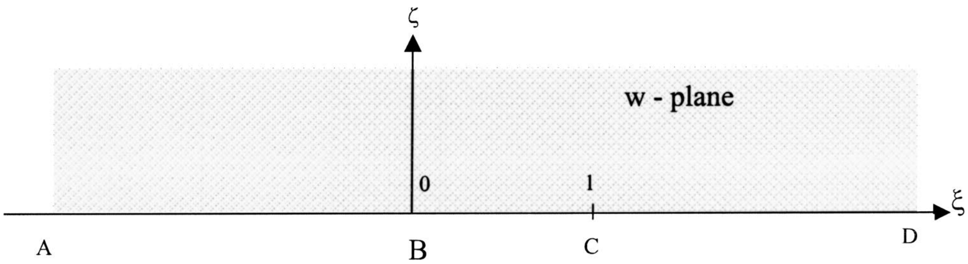

FIG. 2. Physical z plane is conformally mapped onto the upper half of the w plane.

and

$$\gamma_1=\alpha-\beta-\tfrac{1}{2},\quad \gamma_2=\alpha+\beta-\tfrac{1}{2}.$$

Function f_0 is also analytic in the transformed variable w. On the free surfaces, which correspond to $\xi<0$ and $\xi>1$ on the real axis, p_0 vanishes. On the wall surface, which corresponds to the line segment $0<\xi<1$, we take $\partial p_0/\partial n=-a_y$. Therefore, along the real axis in the w plane, we have

$$\mathrm{Re}(f_0)=0 \quad \text{on} \quad -\infty<\xi<0, \tag{21}$$

$$\mathrm{Re}\left(\frac{\partial f_0}{\partial n}\right)=-a_y \quad \text{on} \quad 0<\xi<1, \tag{22}$$

$$\mathrm{Re}(f_0)=0 \quad \text{on} \quad 1<\xi<\infty. \tag{23}$$

If $s(\xi)$ measures the distance from point **C** in Fig. 2 to any point on the wall surface, the Cauchy–Riemann equations give

$$\mathrm{Re}(f_0)=0 \quad \text{on} \quad -\infty<\xi<0, \tag{24}$$

$$\mathrm{Im}(f_0)=-a_y s(\xi) \quad \text{on} \quad 0<\xi<1, \tag{25}$$

$$\mathrm{Re}(f_0)=0 \quad \text{on} \quad 1<\xi<\infty, \tag{26}$$

where the distance $s(\xi)$ is given by (20) as

$$s(\xi)=\frac{(1+\lambda)\Gamma(1+2\alpha)}{\Gamma(1+\gamma_1)\Gamma(1+\gamma_2)}\int_\xi^1 \tau^{\gamma_2}(1-\tau)^{\gamma_1}\mathrm{d}\tau \quad \text{on} \quad 0<\xi<1. \tag{27}$$

If we introduce a new analytic function $g_0(w)$ by

$$g_0(w)=w^{-1/2}(1-w)^{-1/2}f_0(w), \tag{28}$$

the boundary conditions for $g_0(w)$ are unmixed

$$\mathrm{Im}(g_0)=0 \quad \text{on} \quad -\infty<\xi<0, \tag{29}$$

$$\mathrm{Im}(g_0)=-a_y\xi^{-1/2}(1-\xi)^{-1/2}s(\xi) \quad \text{on} \quad 0<\xi<1, \tag{30}$$

$$\mathrm{Im}(g_0)=0 \quad \text{on} \quad 1<\xi<\infty. \tag{31}$$

The analytic function $g_0(w)$ which is regular in the upper half w plane and vanishes at infinity can be obtained from the Schwarz integral formula

$$g_0(w)=\frac{1}{\pi}\int_{-\infty}^{\infty}\frac{\mathrm{Im}(g_0)}{\tau-w}d\tau. \tag{32}$$

Substituting (28)–(31) into (32), we have

$$f_0(w)=-\frac{a_y w^{1/2}(1-w)^{1/2}}{\pi}\int_0^1\frac{s(\tau)}{\tau^{1/2}(1-\tau)^{1/2}(\tau-w)}d\tau. \tag{33}$$

From boundary conditions (13)–(15), we have

$$\eta_{12}(\xi)=-\frac{1}{2}\cos[(\alpha-\beta)\pi]\mathrm{Im}\left(\left.\frac{\partial f_0}{\partial w}\right|_{\zeta=0}\right) \quad \text{on} \quad \xi>1, \tag{34}$$

$$\eta_{22}(\xi)=-\frac{1}{2}\cos[(\alpha+\beta)\pi]\mathrm{Im}\left(\left.\frac{\partial f_0}{\partial w}\right|_{\zeta=0}\right) \quad \text{on} \quad \xi<0. \tag{35}$$

After some mathematical manipulation, we obtain

$$\eta_{12}(\xi)=\frac{a_y\cos[(\alpha-\beta)\pi]}{4\pi}\left[\frac{2\xi-1}{\xi^{1/2}(\xi-1)^{1/2}}\times\int_0^1\frac{s(\tau)}{\tau^{1/2}(1-\tau)^{1/2}(\xi-\tau)}d\tau-2\xi^{1/2}(\xi-1)^{1/2}\times\int_0^1\frac{s(\tau)}{\tau^{1/2}(1-\tau)^{1/2}(\xi-\tau)^2}d\tau\right] \quad \text{on} \quad \xi>1, \tag{36}$$

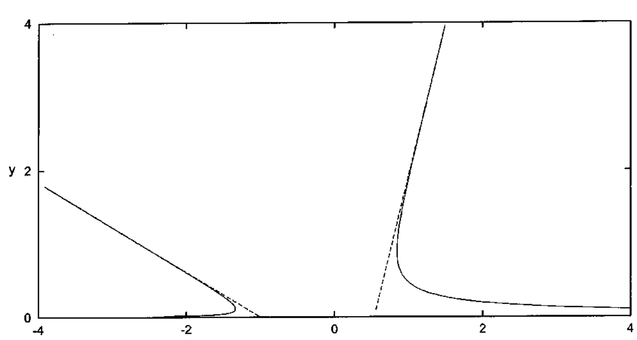

FIG. 3. Impact free-surface profile $\eta_{22}(y)/a_y$ and $\eta_{12}(y)/a_y$ (solid lines) relative to the profile in absence of the wall (dotted lines) for $\alpha=\frac{1}{5}$ and $\beta=\frac{1}{8}$.

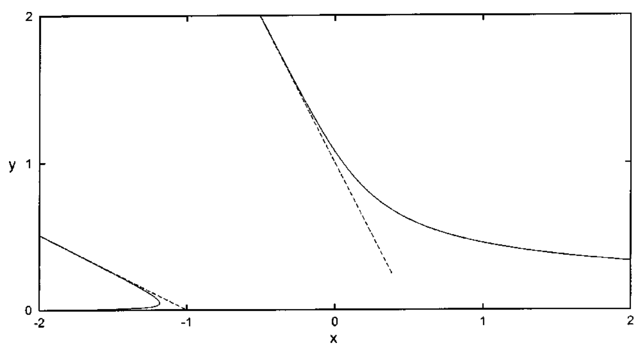

FIG. 4. Impact free-surface profile $\eta_{22}(y)/a_y$ and $\eta_{12}(y)/a_y$ (solid lines) relative to the profile in absence of the wall (dotted lines) for $\alpha=\frac{1}{10}$ and $\beta=\frac{1}{4}$.

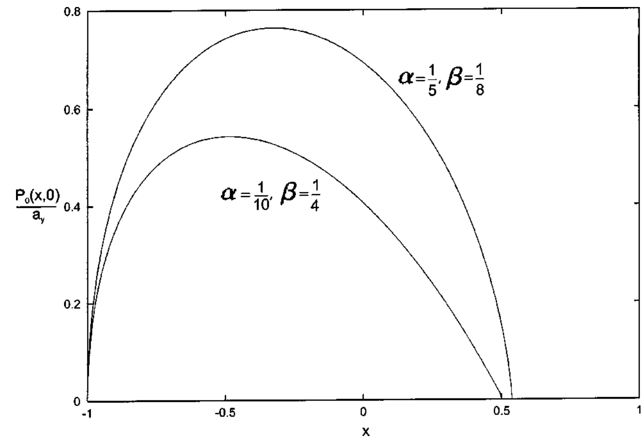

FIG. 5. Impact pressure distributions $p_0(x,0)/a_y$ on the wall for various angle α and β truncated wedge.

$$\eta_{22}(\xi)=-\frac{a_y\cos[(\alpha+\beta)\pi]}{4\pi}\left[\frac{1+2|\xi|}{|\xi|^{1/2}(1+|\xi|)^{1/2}}\times\int_0^1\frac{s(\tau)}{\tau^{1/2}(1-\tau)^{1/2}(\tau+|\xi|)}d\tau-2|\xi|^{1/2}(1+|\xi|)^{1/2}\int_0^1\frac{s(\tau)}{\tau^{1/2}(1-\tau)^{1/2}(\tau+|\xi|)^2}d\tau\right]\quad\text{on}\quad\xi<0. \tag{37}$$

Using (27) and integrating by parts, we have

$$\eta_{12}(\xi)=\frac{a_y\cos(\alpha\pi)\cos(\beta\pi)\Gamma(1+2\alpha)}{\pi\Gamma(\frac{1}{2}+\alpha-\beta)\Gamma(\frac{1}{2}+\alpha+\beta)\xi^{1/2}(\xi-1)^{1/2}}\times\int_0^1\frac{\tau^{\alpha+\beta}(1-\tau)^{\alpha-\beta}}{\xi-\tau}d\tau\quad\text{on}\quad\xi>1, \tag{38}$$

$$\eta_{22}(\xi)=\frac{a_y\cos(\alpha\pi)\cos(\beta\pi)\cos[(\alpha+\beta)\pi]\Gamma(1+2\alpha)}{\pi\cos[(\alpha-\beta)\pi]\Gamma(\frac{1}{2}+\alpha-\beta)\Gamma(\frac{1}{2}+\alpha+\beta)|\xi|^{1/2}(1+|\xi|)^{1/2}}\times\int_0^1\frac{\tau^{\alpha+\beta}(1-\tau)^{\alpha-\beta}}{\tau+|\xi|}d\tau\quad\text{on}\quad\xi<0. \tag{39}$$

Making use of (20), the forms of free-surface profiles $\eta_{12}(y)$ and $\eta_{22}(y)$ close to the wall are seen to be

$$\eta_{12}(y)\to\frac{a_y\cos(\alpha\pi)\cos^2(\beta\pi)\Gamma(1+\alpha+\beta)\Gamma(\alpha-\beta)}{\pi\Gamma(\frac{1}{2}+\alpha-\beta)\Gamma(\frac{1}{2}+\alpha+\beta)}\times\left[\frac{4\cos(\alpha\pi)\Gamma(1+2\alpha)}{(1+2\alpha-2\beta)\Gamma(\frac{1}{2}+\alpha-\beta)\Gamma(\frac{1}{2}+\alpha+\beta)}\right]^{1/(1+2\alpha-2\beta)}y^{-1/(1+2\alpha-2\beta)}+O(y^{1/(1+2\alpha-2\beta)})\quad\text{as}\quad y\to0, \tag{40}$$

$$\eta_{22}(y)\to\frac{a_y\cos(\alpha\pi)\cos^2(\beta\pi)\cos[(\alpha-\beta)\pi]\Gamma(1+\alpha-\beta)\Gamma(\alpha+\beta)}{\pi\cos[(\alpha-\beta)\pi]\Gamma(\frac{1}{2}+\alpha-\beta)\Gamma(\frac{1}{2}+\alpha+\beta)}\times\left[\frac{4\cos(\alpha\pi)\cos[(\alpha+\beta)\pi]\Gamma(1+2\alpha)}{(1+2\alpha+2\beta)\cos[(\alpha-\beta)\pi]\Gamma(\frac{1}{2}+\alpha-\beta)\Gamma(\frac{1}{2}+\alpha+\beta)}\right]^{1/(1+2\alpha+2\beta)}y^{-1/(1+2\alpha+2\beta)}+O(y^{1/(1+2\alpha+2\beta)})\quad\text{as}\quad y\to0. \tag{41}$$

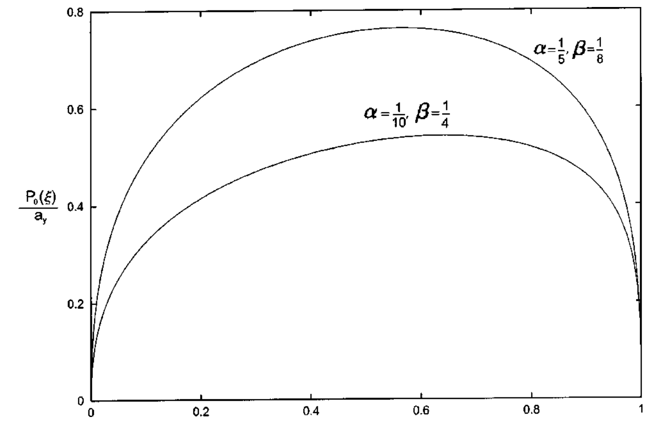

FIG. 6. Impact pressure distributions $p_0(\xi)/a_y$ on the wall for various angle α and β truncated wedge.

Impact free-surface profiles for various α and β are shown in Figs. 3 and 4. It has been found that the free-surface profiles $\eta_{12}(y)$ and $\eta_{22}(y)$ close to the wall are proportional to $y^{-1/(1+2\alpha-2\beta)}$ and $y^{-1/(1+2\alpha+2\beta)}$, respectively, which are neither linear in Cumberbatch's assumption[1] nor exponential in Zhang *et al.*'s assumption.[2]

The impact pressure on the wall is the real part of $f_0(w)$ for $0<\xi<1$. Using (27) and (33) and integrating by parts, we have on $0<\xi=\sin^2\phi<1$, $0<\phi<\pi/2$

$$p_0(\xi)=\mathrm{Re}(f_0|_{\zeta=0}) = \frac{2a_y(1+\lambda)\Gamma(1+2\alpha)}{\pi\Gamma(1+\gamma_1)\Gamma(1+\gamma_2)} \times\int_0^{\pi/2}\sin^{\alpha+\beta}\theta\cos^{\alpha-\beta}\theta\ln\left|\frac{\sin(\theta+\phi)}{\sin(\theta-\phi)}\right|d\theta. \quad (42)$$

Figures 5 and 6 show clearly that the maximum impact hydrodynamic pressure always appears near the center of the fluid truncated wedge.

IV. CONCLUSIONS

The problems of oblique breaking waves impingement on the wall and the free-surface profiles have been solved analytically by using a small-time expansion. The results obtained show that the free-surface profiles can be determined if the angles and acceleration of the oblique breaking wave are given. The results of this paper agree with the results of the case of a normal impact (Shu[3]) with angle $\beta=0$. In addition, we have further confirmed that the free-surface profile close to the wall is neither linear in Cumberbatch's assumption[1] nor exponential in Zhang *et al.*'s assumption.[2]

ACKNOWLEDGMENTS

The author is grateful to Professor L. Gary Leal and the reviewers for their constructive comments and suggestions.

[1] E. Cumberbatch, "The impact of a water wedge on a wall," J. Fluid Mech. **7**, 353 (1960).
[2] S. Zhang, D. K. P. Yue, and K. Tanizawa, "Simulation of plunging wave impact on a vertical wall," J. Fluid Mech. **327**, 221 (1996).
[3] J.-J. Shu, "Impact of breaking wave on a wall," Proceedings of the International Conference on Applied Mathematics & Mathematical Physics, Sylhet, Bangladesh, 2000.
[4] A. T. Chwang, "Hydrodynamic pressures on sloping dams during earthquakes. Part 2. Exact theory," J. Fluid Mech. **87**, 343 (1978).
[5] A. T. Chwang, "Nonlinear hydrodynamic pressure on an accelerating plate," Phys. Fluids **26**, 383 (1983).
[6] P. L.-F. Liu, "Hydrodynamic pressures on rigid dams during earthquakes," J. Fluid Mech. **165**, 131 (1986).
[7] A. C. King and D. J. Needham, "The initial development of a jet caused by fluid, body and free-surface interaction. Part 1. A uniformly accelerating plate," J. Fluid Mech. **268**, 89 (1994).